Title:

Inactivity-mediated molecular adaptations: Insights from a novel pre-clinical model of physical activity reduction

Authors:

Alice Meyer[1], Nicole Kim[2], Melissa Nguyen[3], Monica Misch[2], Kevin Marmo[2], Jacob Dowd[3], Christian Will[2], Milica Janosevic[2], Erin J Stephenson[1,2,4,5,6]

Affiliations:

1. Department of Anatomy, College of Graduate Studies, Midwestern University, Downers Grove, IL 60515, U.S.A.
2. Chicago College of Osteopathic Medicine, Midwestern University, Downers Grove, IL 60515, U.S.A.
3. Department of Biomedical Science, College of Graduate Studies, Midwestern University, Downers Grove, IL 60515, U.S.A.
4. Physical Therapy Program, College of Health Sciences, Midwestern University, Downers Grove, IL 60515, U.S.A.
5. Physician Assistant Program, College of Health Sciences, Midwestern University, Downers Grove, IL 60515, U.S.A.
6. College of Dental Medicine Illinois, Midwestern University, Downers Grove, IL 60515, U.S.A.

Running head:

Transcriptional responses to physical activity reduction

Corresponding Author:

Erin J Stephenson, Ph.D.
Assistant Professor, Department of Anatomy,
College of Graduate Studies
Midwestern University
Science Hall 542L,
555 31st Street,
Downers Grove, IL 60515, U.S.A.
estephenson@midwestern.edu

Abstract

Insufficient physical activity is associated with an increased relative risk of cardiometabolic disease and is an independent risk factor for mortality. Experimentally reducing physical activity in humans and animals rapidly induces insulin resistance, impairs glucose handling, and drives metabolic inflexibility. These metabolic adaptations manifest during the early stages of physical activity reduction, even when energy balance is maintained, suggesting that inactivity-mediated metabolic reprogramming is an early event that precedes changes in body composition and other more obvious signs of metabolic disease. To identify mechanisms that promote the aberrant metabolic adaptations associated with physical inactivity, we developed a novel mouse model of physical activity reduction that allowed us to study the effects of physical activity reduction prior to the onset of overt changes in body composition. Ten-week-old female and male C57BL6/NJ mice were randomized into three groups: an inactive control group (standard rodent housing, n=10-11), an active control group (treadmill running 5 d/week at 70% of maximal running speed for 30 min/d over 6-weeks, n=11-11), and an activity reduction group (treadmill running for 4-weeks, followed by 2-weeks of inactivity, n=9-11). Transcriptional profiling in gastrocnemius muscle identified seven transcripts uniquely altered by physical activity reduction compared to the inactive and active control groups, most of which have reported functions linked to bioenergetic adaptation. Future studies will provide deeper characterization of the function(s) of each the seven transcripts we identified as being uniquely altered by physical activity reduction in skeletal muscle while also identifying how inactivity affects transcriptional regulation in other tissues.

New and noteworthy

We generated a novel treadmill-based model of physical activity reduction that acknowledges the need for research animals to be more active than typical laboratory housing permits, but not so active the active period no longer represents activity levels achievable for most humans. Leveraging this model in the presence of both an active and inactive control group, we used transcriptional profiling to identify seven transcripts uniquely altered by physical activity reduction in skeletal muscle.

Key words

Physical inactivity, physical activity reduction, skeletal muscle metabolism, skeletal muscle transcriptome

Introduction

Physical inactivity is one of the leading risk factors for mortality, contributing to >7% of all-cause and cardiovascular deaths annually(1). The global health burden of physical is driven by a relationship between physical inactivity and an increased relative risk of developing a suite of non-communicable diseases such as type-2 diabetes, coronary heart disease, stroke, dementia, and several types of cancer(1, 2). Despite the well-established benefits of regular physical activity on overall health and well-

being, approximately one third of the adult population and 81% of adolescents globally do not meet the minimum level of physical activity required for health (i.e., 60 minutes/day of moderate intensity aerobic activities on at least 3 days/week for children and adolescents or 150 minutes/week of moderate intensity aerobic activity for adults)(3-9). In most regions of the world the prevalence of physical inactivity is greatest in girls and women(8-10), while among adults who are classified as being physically inactive, older adults are disproportionately affected(2). Thus, there is a large global population that would benefit from increasing their physical activity levels. Unfortunately, an increasing number of individuals face barriers that prevent them from engaging in exercise for its health benefits(11), thus the prevalence of physical inactivity(1, 12) and inactivity-related disease(13-15) continues to increase.

The past two decades has seen a strong push toward characterizing the physiology of physical inactivity to identify how inactivity drives disease(16-18). This necessary first step has identified a core suite of metabolic adaptations common across multiple models of physical activity reduction. Step reduction(19-24) and bedrest(25-31) protocols in humans and wheel lock(32-39) and cage size reduction(40-43) protocols in animals demonstrate that a reduction in physical activity rapidly induces insulin resistance, impairs glucose handling and drives metabolic inflexibility. These early metabolic adaptations manifest even when energy balance is maintained(25, 27), suggesting inactivity-mediated metabolic reprogramming precedes changes in body composition. However, despite a growing interest in understanding the physiology of physical inactivity, our knowledge of the molecular mechanisms that facilitate metabolic adaptations caused by physical inactivity remains limited.

Our ability to identify the mechanisms responsible for inactivity physiology has been limited, in part, by how we model physical inactivity in preclinical settings. Most laboratory animals are housed in environments that restrict activity while concurrently providing free and continuous access to food. Such housing conditions are thought to render animals metabolically morbid making them unsuitable for use as physically active control animals when strategies that further reduce physical activity are employed (i.e., cage size reduction or hind limb casting/unloading)(44). In contrast, while wheel lock models do address the need for animals to be active prior to initiating activity reduction, voluntary wheel running poses its own limitations, such as not being able to easily control the duration and/or intensity of physical activity animals undertake during the active phase of the protocol.

Acknowledging the utility and limitations of existing animal models of physical activity reduction, we have developed a new treadmill-based rodent model of physical activity reduction. Our protocol involves an initial active phase where exercise intensity, duration, and time of day can be tightly controlled, followed by an inactive phase that reduces physical activity without shrinking home cage size or inhibiting hindlimb mobility. Here, we describe this new model of physical activity reduction alongside both inactive and active control animals and report the transcriptional changes uniquely caused by physical activity reduction in skeletal muscle. We hypothesized that physical activity reduction would cause a unique transcriptional response compared to both active and inactive control animals and that

the differentially expressed transcripts associated with physical activity reduction would have functions linked to metabolism.

Materials and methods

Animals, housing, diet

Female and male C57BL/6NJ mice (strain #005304) were purchased from The Jackson Laboratory at nine weeks-of age ±3 days. Upon arrival at the Midwestern University Animal Facility, mice were housed in a temperature- and humidity-controlled environment (22.2°C, 40% relative humidity) in 7.5”W x 11.5”L x 5”H cages (Ancare #N10) containing corn cob bedding and standardized enrichment (i.e., a plastic tunnel and an iso-BLOX square). Animals were maintained on a 12:12 h light:dark photoperiod cycle and unless otherwise specified, mice had free access to food (Teklad Global #2918; 24% kCal from protein, 18% kCal from fat, 58% kCal from carbohydrate, 3.1 kCal/g) and autoclaved tap water at all times. Throughout the study period, mice were weighed twice weekly using a precision balance under dynamic weighing conditions (Mettler Toledo #MS1602TS). The Midwestern University Institutional Animal Care and Use Committee approved all animal procedures in advance of the study (protocol #3180).

Treadmill setup and acclimation procedure

All treadmill exercise was conducted on a 5-Lane Touchscreen Convertible Treadmill (Panlab Harvard Apparatus #76-0896) set at a 15° incline. Mice were initially acclimated to the treadmill by placing them on the stationary belt for ~5 minutes, after which time the belt was started at a speed of 6 m/min. Belt speed was progressively increased in increments of 0.6 m/min every minute until mice were running at a speed of 10 m/min, which they maintained for 5 minutes before being returned to their home cages. This acclimation protocol was repeated up to three times (separate days for each occurrence).

Physical activity reduction protocol

Ten-week-old mice were randomized into one of three groups (Figure 1a). One group remained inactive (i.e., typical shoe-box style housing with standard enrichment; inactive control group). A second group completed daily treadmill running sessions 5 d/week for 6 weeks (active control group), and a third group completed daily treadmill training 5 d/week for 4 weeks followed by two weeks of inactivity (activity reduction group). Each training session involved a 10-minute warm up period (5 min at 6 m/min, then 5 min at 10 m/min), followed by up to 30 minutes at ~70% of maximal running speed (predetermined during the prior graded maximal running test, described below; Figure 1b). Duration spent running at 70% of maximal running speed was progressively increased from an initial 15 min to 30 min during the first three weeks of the training program and remained at 30 min/d thereafter (for a total of 40 min running per training session; Figure 1c). To promote training adaptations, running speed was increased by 5% after the first two weeks of training. After 4 weeks, graded maximal running tests were repeated and training

speed was adjusted to 70% of the new maximal running speed. All training sessions were conducted between ZT 8-10 h. When necessary, mice were encouraged to run using vocal cues, bursts of compressed air, and/or use of a physical probe to gently tap their hindquarters.

Graded maximal running tests

Maximal running capacity was assessed at the beginning, after 4 weeks, and end of the study using graded maximal running tests. Mice were placed onto a stationary treadmill for up to 5 minutes after which the belt was started at a speed of 6 m/min. Mice maintained this speed for 2 min at which point the speed increased an additional 2 m/min every 2 min until mice reached exhaustion. Exhaustion was defined as the point when a mouse could no longer maintain a running pace that matched the speed of the treadmill and/or they refused to continue running despite gentle encouragement from the person(s) administering the test (as described above). Maximal speed, running distance and running time were recorded. Work during each stage of the test was calculated and summed to determine the total work performed during each test. Work was calculated as: Work J = Force [Body mass kg x 9.18 N] x Vertical Distance [Speed m/sec x Incline (fractional grade) x Time sec].

Food intake

During the fifth week (i.e., after >1 week of inactivity for the activity reduction group), food intake of individual mice was determined. To facilitate measurement of food intake, mice were moved in pairs into 7.625W” x 15.01”L x 5.13”H cages (Allentown #223581-4) with duel external bottle cage tops (Allentown #228843-1), stainless steel half pocket wire feeders (Allentown #314677) retrofitted with stainless steel dividers, and perforated plastic central dividers that physically separated mice and their food and water access points from one another while retaining many of the social aspects of group housing (Allentown #224520-1). Mice were provided with known amounts of food from which daily consumption was calculated based on the weight of food remaining on subsequent days. Energy intake was calculated by multiplying the grams of food eaten by the energy density of the diet (3.1 kCal/g).

Bomb calorimetry

Stool was collected from cages following the final day of food intake monitoring and stored at -80°C. To prepare samples for calorimetry, stool was dried at 70°C in an oven overnight before being pressed into a single pellet of at least 25 mg using a pellet press. For each sample a 10 cm wire fuse was coiled, placed above the stool pellet and connected to the terminals of the calorimeter (6725 Semimicro Calorimeter, Parr). The bomb chamber was then filled with O_2 to a pressure of 35 atm and stool pellets were combusted. Energy released during combustion was recorded.

Tissue collection

Mice were allowed to recover for 48-72 h following the final maximal running test after which they were fasted for 4-6 hours starting at the beginning of the light photoperiod. Mice were anesthetized with isoflurane and blood was collected from the retroorbital sinus using a heparinized capillary and placed immediately on ice. Fasting blood glucose concentrations were measured using a hand-held glucometer (Contour next ONE). Vaginal lavage with sterile PBS was performed on female mice to collect cells for microscopic identification and subsequent determination of estrous stage(45). Following blood collection, anesthetized mice were euthanized by cervical dislocation and tissues rapidly dissected. Right hindlimb muscles were immediately dissected out whole and freeze clamped between stainless steel paddles precooled in liquid nitrogen. Right hindlimb muscles (tibialis anterior and the quadriceps and triceps surae complexes) were carefully dissected out whole and weighed. The left inguinal, gonadal (periuterine or epididymal) and retroperitoneal adipose depots were carefully dissected out and weighed as indices of adiposity.

Insulin ELISA and HOMA-IR

Fasting blood collected from the retroorbital sinus was allowed to rest on ice for at least 30 min before being centrifuged at 1000 RCF for 20 min at 4°C. Following separation of plasma from the cellular blood components, the plasma was moved into fresh tubes, snap frozen and then stored at -80°C. Frozen plasma was thawed over ice and an ELISA was performed on samples and known standards in triplicate according to the manufacturer's instructions for a wide-range assay (Crystal Chem #90080). Absorbance was read at 450 nm with background correction for absorbance at 630 nm (Spectramax iD5, Molecular Devices). Fasting plasma insulin concentrations and fasting blood glucose concentrations were used to calculate the Homeostasis Model Assessment of Insulin Resistance (HOMA-IR) using the equation: HOMA-IR = [fasting insulin (μU/mL) x fasting glucose (mmol/L)] / 22.5.

Glycogen determination in skeletal muscle

The quadriceps muscle complex was powdered while frozen using a liquid nitrogen cooled mortar and pestle. Samples were placed in screw cap vials containing 30% KOH and boiled at 95 °C for 30 minutes with occasional mixing. Samples were then cooled, and 1 M sodium sulfate and 100% ethanol were added. Samples were boiled again for 5 minutes before being centrifuged at 13,000 RCF for 5 minutes at room temperature. After discarding the supernatant, any residual glucose remaining on the glycogen pellet was washed away by resuspending the pellet in water, adding ethanol, and centrifuging the tubes to re-pellet the glycogen. The wash step was repeated three times. Glycogen pellets were allowed to dry at room temperature before being digested overnight at 37°C in 0.3 mg/mL amyloglucosidase prepared in 50 mM sodium acetate, pH 4.8. The next morning, the amount of glucose derived from glycogen was quantified using a commercial glucose kit (Glucose Autokit, Wako diagnostics).

RNA isolation

RNA was extracted from the entire medial belly of the gastrocnemius muscles. Muscles underwent bead homogenization in Trizol. Chloroform was then added to each tube and homogenates were mixed and centrifuged at 4°C to separate the RNA from DNA and protein. RNA was collected from the upper phase and column purified using a commercial kit (PureLink RNA mini kit). RNA concentrations and quality were estimated spectrophotometrically (NanoDrop, ThermoFisher Scientific). RNA quality was determined by denaturing agarose gel electrophoresis(46).

cDNA library prep and transcriptomics

Aliquots of RNA were sent for commercial sequencing (Azenta). Briefly, RNA integrity was verified by TapeStation (RIN range 8.8-9.8). RNA then underwent Poly(A) selection and cDNA libraries were prepared. Paired end bulk RNA seq was performed (Illumina). Data processing and analysis was completed in house as follows: FASTQ files were imported into Galaxy(47) and sequencing data were trimmed (fastp(48)), aligned to genome assembly GRCm39 (RNA STAR(49)), and reads mapped (featureCounts(50)). Count normalization and differential expression analysis was performed using DESeq2[47] in R. Transcripts were considered differentially expressed when FDR<0.05 and the fold change was >0.25 in either direction. Gene Set Enrichment Analysis (GSEA) was also performed (fgsea(51)) using the Gene Ontology Biological Processes reference gene set which was downloaded from Molecular Signatures Database(52-54). Enrichment of gene sets is reported where FDR<0.25.

Statistics

Time course data were analyzed by linear mixed models with likelihood ratio tests and (if applicable) inclusion of fixed factors in the models (see figure legends for details specific to each case), followed by pairwise comparisons using the estimated marginal means to identify differences between individual groups. Single timepoint data were assessed for homoskedasticity using Levene tests and for normality using Shapiro-Wilk tests. Data that met parametric assumptions were analyzed by either one-way ANOVA with post-hoc Tukey tests or ANCOVA. Non-parametric data were analyzed using Kruskal-Wallis tests with post-hoc Dunn tests. Data wrangling, statistical analyses, and data visualization were performed using R v4.4.1 in R Studio build 764 using the following packages: tidyverse v2.0.0 (55), car v3.1-2(56), rcompanion v2.4.36(57), rstatix v0.7.2(58), lme4 v1.1-35.5(59), and emmeans v1.10.4(60).

Results

Running capacity

To ensure that the treadmill training protocol we employed was sufficient to induce a training effect, graded maximal running tests were performed at 0-, 4- and 6-weeks and the amount of work performed during each test was determined (Figure 1d). Group effects were identified for both female (p=0.003) and

male mice (p=0.043), with mice in the Active groups performing more overall work than mice in the Inactive groups (p=0.003 for female and p=0.044 for male mice). In contrast, work performed by the Activity Reduction groups was not different from that of the Active (p=0.491 for female and p=0.305) or Inactive groups (p=0.078 for female and p=0.578 for male mice). These findings indicate that not only was the training protocol we employed sufficient to improve performance in both female and male mice, but also that two weeks of inactivity following a four-week training period was sufficient for reversing the effects of regular physical activity on performance.

Body mass

One of the goals we had when developing our novel model of activity reduction was to be able to collect data after a period of reduced activity that was sufficient to ensure we weren't simply measuring the effects of recovering from the last exercise bout, but also wasn't so long as to be confounded by significant body mass gains. To this end, we chose a two-week period of inactivity for our Activity Reduction groups and closely tracked body mass throughout the study. Over the duration of the study, no differences in body mass were observed between groups for either sex (Figure 1e; p=0.895 for female and p=0.505 for male mice), despite Active male mice appearing to weigh less than either the Inactive or Activity Reduction groups at the end of 6-weeks (p=0.220). The amount of body mass gained after the first four weeks also did not differ between groups for either sex (Figure 1f; p=0.974 for female and p=0.335 for male mice). However, between the fourth and sixth weeks, body mass gained by male mice was different between groups (Figure 1g, p=0.003), with male mice in the Activity Reduction group having gained 167.5% more body mass than the Active group during this period (p=0.002). The Inactive males also appeared to gain more body mass than the Active males; however, this did not meet the a priori threshold for statistical significance (82.1%, p=0.165). Similarly, although the Activity Reduction males gained 46.9% more body mass compared to the Inactive males, this difference did not meet requirements for statistical significance either (p=0.143). No differences were detected between groups for body mass gained between weeks four and six for female mice (p=0.276). Together, these data indicate that although two weeks of activity reduction does not lead to a meaningful body mass divergence overall, activity reduction does rapidly reverse the effects of being physically active on suppressing body mass gains in male mice.

Adipose and skeletal muscle mass

Increases in adiposity and decreases in lean mass have been widely reported to occur in response to physical activity reduction(27, 32, 34, 37, 41). Given these reports and our observation that male mice in the Activity Reduction group experienced catch up weight gain during the two-week inactive phase of the study, we sought to determine whether our Activity Reduction protocol led to changes in the mass of a selection of adipose tissue depots and hind limb skeletal muscles (Figure 1h). For female mice, no

differences were observed between groups for the mass of the inguinal, retroperitoneal, or periuterine adipose depots (p=0.744, p=0.481, and p=0.365, respectively). For male mice, the Active group appeared to have less adipose mass in their inguinal, retroperitoneal, and epididymal depots when compared to males in the Inactive (-31.4%, -42.0%, and -37.7%, respectively) and Activity Reduction groups (-20.4%, -36.6%, -20.6%, respectively). However, criteria for statistical significance were not met for any of the measured depots (p=0.082, p=0.077, and p=0.074, respectively). Since both body mass and the mass of the individual adipose depots were highly variable within individual groups, we repeated the comparison with the inclusion of body mass at the time of tissue collection as a covariate in a secondary analysis of the male mice. However, even with body mass included as a covariate, no differences were detected between groups for either the inguinal, retroperitoneal, or epididymal depots (p=0.112, p=0.140 and p=0.094, respectively). In both female and male mice, no differences between groups were observed for the mass of the quadriceps complex (p=0.256 and p=0.935, respectively) or the tibialis anterior muscle (p=0.776 and p=0.678). The triceps surae complex was also similar in mass across groups for male mice (p=0.612); however, in female mice that were Active and those that underwent Activity Reduction, the triceps surae complex weighed less than that of the females in the Inactive group (12.9%, p=0.020 and 12.9%, p=0.020, respectively). Although limited by the adipose depots and hindlimb muscles chosen for comparison, these data suggest that two-weeks of Activity Reduction may alter body composition in a sexually dimorphic and tissue-specific manner.

Energy intake and absorption

Following our observation that male mice experienced catch up body mass gains during the two-week activity reduction period, we sought to determine whether any differences in body mass might be associated with changes in energy intake (Figure 2a) or energy absorption from the diet (Figure 2b). We observed a group effect for energy intake in Female mice (p=0.034), but not male mice (p=0.876). Female mice in the Activity Reduction group consumed 32.6% more energy per day than females in the Inactive group (p=0.028). Female mice in the Active group also appeared to have greater daily energy intake than those in the Inactive group; however, this did not meet a priori criteria for statistical significance (21.5%, p=0.186). No differences in energy intake were observed between female mice in the Active and Activity Reduction groups (p=0.618). We also measured the energy excreted in the stool using bomb calorimetry as a surrogate measure of energy absorption from the diet (Figure 2b). No differences were observed between groups in either female (p=0.941) or male mice (p=0.438), suggesting that activity reduction had little effect on energy absorption. These findings suggest that in female but not male mice, being active likely regulates energy intake, an effect that persists into the first two weeks of activity reduction. Considering these observations alongside our earlier finding that activity reduction did not lead to differences in body mass or energy absorption in female mice, it's tempting to extrapolate these results to suggest that energy expenditure was likely greater in female mice in the Active and Activity Reduction

groups compared to the Inactive group. In contrast, given that male mice in the Activity Reduction group were experiencing catch up weight gain during the period we measured energy intake and absorption, and our observation that male mice across all three groups consumed and absorbed similar amounts of energy, we predict that male mice in the Activity Reduction group would have reduced energy expenditure compared to the Active and Inactive groups. Unfortunately, the experimental design used in this study does not allow for the accurate measurement of daily energy expenditure using indirect calorimetry. Thus, future studies using this model of activity reduction will need to consider alternative approaches to tease out the effects of activity reduction on energy expenditure and determine the if there are any sex-specific responses.

Fasting insulin, glucose, and HOMA-IR

To determine whether two-weeks of activity reduction was sufficient to induce hyperinsulinemia, hyperglycemia, insulin resistance, or other disruptions in glucose homeostasis that have been previously reported in other models of activity reduction(20-29, 31, 39, 40, 43, 61), we measured fasting plasma insulin (Figure 3c), fasting blood glucose concentrations (Figure 3d), and calculated the HOMA-IR index (Figure 3e). In both female and male mice, neither fasting insulin concentrations ($p=0.304$ and $p=0.782$, respectively) nor fasting glucose concentrations were different between groups ($p=0.860$ and $p=0.808$, respectively). HOMA-IR was also not different for either female or male mice ($p=0.197$ and $p=0.932$, respectively), despite female mice in the Activity Reduction group appearing to have a somewhat greater HOMA-IR than either the Active (32.8%, $p=0.208$) or Inactive groups (41.2%, $p=0.316$). These findings suggest that two-weeks of activity reduction was not sufficient to induce overt disruptions in systemic glucose homeostasis, at least not when animals are in a fasted state.

Muscle glycogen concentrations

Since skeletal muscle is a major organ of glucose uptake and storage in the form of glycogen, and a recent study indicated that bed rest in humans leads to increased muscle glycogen storage(61), we also measured glycogen concentrations in the quadriceps muscle complex (Figure 3f). A group effect was observed for female mice ($p=0.037$), which was explained by female mice in the Activity Reduction group having 67.6% more muscle glycogen than female mice in the Inactive group ($p=0.035$). Muscle glycogen concentrations in the Active group also appeared to be greater than those of the Inactive group, but this difference did not meet a priori assumptions for statistical significance (52.7%, $p=0.124$). In contrast, although male mice in the Active group appeared to have greater muscle glycogen concentrations than the Inactive (31.5%) or Activity Reduction groups (25.2%), no group effects were detected ($p=0.292$). These findings indicate that two-weeks of physical activity reduction results in sexually dimorphic responses to muscle glycogen concentrations.

Transcriptional adaptations to activity reduction in skeletal muscle

A major goal of this study was to perform transcriptional profiling in tissues from mice that underwent our novel activity reduction paradigm in the hopes of identifying transcripts uniquely changed in response to activity reduction compared to both active and chronically inactive control groups. Bulk RNAseq was performed on RNA isolated from the medial belly of the gastrocnemius muscles from female mice (Figure 4). The Active group had 71 differentially expressed transcripts compared to the Inactive group (Figure 4a), whereas the Activity Reduction group had 40 differentially expressed transcripts compared to the Inactive group (Figure 4b). Compared to the Active group, the Activity Reduction group had 124 differentially expressed transcripts (Figure 4c). After identifying the differentially expressed transcripts in each comparison, we next identified which of the differentially expressed transcripts either overlapped between or were unique to each comparison (Figure 4d). Using this approach, we identified seven transcripts that were uniquely changed in the Activity Reduction group compared to both the Active and Inactive groups (Figure 4e). Of these transcripts, *Smyd2*, *En1*, and *Hoxa11os* were all increased in expression following Activity Reduction, whereas *Ostn*, *Ak4*, *Srrm4os*, and *Zfhx4* were all decreased in expression. One transcript, *Igfbp5*, was decreased in both the Active and Activity Reduction groups compared to the Inactive group (Figure 4f). Sixteen transcripts were differentially expressed in the Active group compared to both the Inactive and Activity Reduction group (Figure 4g), with the Active group having increased expression of *Acly*, *Cd209f*, *Elovl6*, *F13a1*, *Folr2*, *Fndc1*, *Gfpt2*, *Gimap6*, *Il1r1*, *Lama4*, *Nrp2*, *Rassf2*, and *Spred1* and decreased expression of *Ctxn3*, *Dglucy* and *Gstp2*.

Gene set enrichment analysis was also performed against the Gene Ontology Biological Processes curated gene set (Supplementary File 1). 76 gene sets were positively enriched in the Active group compared to the Inactive group. Of these 76 gene sets, all were found to be negatively enriched in the Activity Reduction group when compared to the Active group, suggesting that enrichment of these pathways is dependent on regular physical activity and two weeks of physical activity reduction is sufficient to reverse the activity mediated adaptations. Pathways identified were involved in immune and stress responses, vasculature development and angiogenesis, wound repair, metabolism, and signal transduction. In addition to the pathways found to be positively enriched in response to activity and negatively enriched in response to activity reduction, seven other pathways were identified as being negatively enriched by activity reduction compared to the active group. These include *Endocytosis*, *Import into Cell*, *Vesicle mediated transport*, *Regulation of vesicle mediated transport*, *Regulation of catalytic activity*, *Positive regulation of catalytic activity*, and *Positive regulation of molecular function*. No pathway enrichment was observed when comparing the Activity Reduction group to the Inactive group.

Discussion

Here, we report a new animal model of physical activity reduction that acknowledges the need for animals to be active prior to initiating inactivity, but not so active that they no longer represent daily activity levels

typically achieved by humans. Our model improves upon existing models of activity reduction, such as the cage size reduction(40-43) and wheel lock models(33, 62), by allowing investigators to control the exercise intensity, exercise duration, and time of day that animals are active. This ensures the activity dose received by both the active control group and the activity reduction group (prior to initiation of inactivity) is consistent and at a volume that translates to levels achievable in everyday life for most humans. Since traditional exercise training paradigms designed for increasing performance in humans typically involve exercising at 70% of maximal heart rate or 70% of maximal load, we chose a 10 min low speed warm up followed by 70% of maximal running speed for 30 min per day, 5 d per week as a physiologically meaningful workload for the training phase of our protocol. This approach resulted in performance adaptations following the initial four-week training phase that then regressed to levels of the inactive control group following the two-week period of activity reduction. Furthermore, by limiting the activity reduction phase to two-weeks and including both active and inactive control groups in the experimental design, we were largely able to study the molecular effects of physical activity reduction without the confounding influence of overt differences in body mass or body composition.

Using this new model, we identified seven transcripts in skeletal muscle that were uniquely changed in response to physical activity reduction. Notably, these changes were identified after all mice, regardless of group assignment, had all undergone one final exercise bout (i.e., the 6-week timepoint graded maximal running test) and had been allowed to recover from the acute effects of exercise before tissues were collected. This suggests that changes in the expression of the identified transcripts were indeed driven by the two-week period of activity reduction and less likely to be caused by sampling tissues during the initial recovery period that follows an acute bout of exercise.

Smyd2, *En1*, and *Hoxa11os* were all increased in expression in response to activity reduction. Of these three transcripts, *Smyd2* was by far the most highly expressed. *Smyd2* encodes the lysine methyltransferase SET [Su(Var)3-9, Enhancer-of-zeste and Trithorax] and MYND [Myeloid, Nervy, and DEAF-1] domain containing 2 (SMYD2). SMYD2 monomethylates lysine residues on both histone and non-histone proteins(63) and has largely been studied in the context of tumor biology. Outside of cancer field, SMYD2 has been reported to play a role in regulating titin stability in striated muscle(64, 65). More recently SMYD2 has been found to increase in abundance in the skeletal muscle and livers of hibernating animals during the early stages of torpor(66, 67), providing further evidence that SMYD2 is induced when levels of physical activity are suddenly reduced. Given that SMYD2 has also been linked to the development of metabolic-associated steatotic liver disease(68), we predict that SMYD2 plays a role in regulating metabolic adaptations caused by sudden reductions in bioenergetic demand. Indeed, based on findings in cervical cancer cell lines(69) and our own data (not shown, manuscript forthcoming), *Smyd2* induction in response to reductions in physical activity is likely linked to changes in the way glucose and glucose-products are handled by skeletal muscle.

Although basal expression is much lower in skeletal muscle, *En1*, and *Hoxa11os* were also

induced by activity reduction. *En1* encodes engrailed 1 (EN1), which has been shown to bind and regulate the expression of utrophin(70). *En1* has also been linked to pro-fibrotic TGFβ signaling(71, 72), is highly expressed in dopaminergic neurons(73), and has been negatively associated with the thermogenic- and positively associated with the lipogenic capacities of brown adipocytes(74). Less is known about the function of the long non-coding RNA *Hoxa11os*. However, in colon cells, *Hoxa11os* localizes to mitochondria and interacts with several core mitochondrial proteins involved in bioenergetic functions(75). Thus, although our understanding of the function of *En1* and *Hoxa11os* in skeletal muscle is currently limited, these reports suggest *En1* and/or *Hoxa11os* induction in response to activity reduction could be linked to inactivity-associated mitochondrial adaptations in one or more of the cell populations present in skeletal muscle.

Of the transcripts that were decreased in expression following activity reduction, *Ostn* had the highest basal expression. *Ostn* encodes a the musclin protein (also known as osteocrin), a known myokine that acts as an agonist for natriuretic peptide receptors(76). *Ostn*/musclin induction in skeletal muscle is linked to energy availability, with *Ostn*/musclin expression found to be lower during fasting and higher upon refeeding(76). *Ostn*/musclin is also induced acutely in response to treadmill running(77), indicating that it is exercise-responsive and may contribute to adaptations associated with regular exercise. In line with this notion, when *Ostn*/musclin is absent, impairments in exercise capacity are observed, a finding thought to be due to musclin's purported influence over mitochondrial biogenesis(77). Conversely, musclin has been identified as a negative regulator of adipocyte thermogenesis(78), and high basal *Ostn*/musclin expression has been reported in animals and people with obesity, insulin resistance, and type-2 diabetes(78-81). In the present study, the expression of *Ostn* was reduced in response to physical activity reduction, as was overall exercise capacity compared to the Active control group. Although merely an association, given previous reports regarding the function of *Ostn*/musclin with regards to exercise tolerance(77), and its role in exercise-mediated cardiac conditioning(82), it is possible that inhibition of *Ostn*/musclin is required for reversal of the effects of regular exercise on functions linked to exercise performance. Whether reductions in *Ostn* expression are associated with changes in circulating musclin concentrations, and whether low *Ostn* expression persists after longer periods of inactivity and/or once significant changes in body composition set in remains to be determined.

Ak4, *Srrm4os* and *Zfhx4* were also all decreased in expression in response to activity reduction, although their basal expression was much lower than *Ostn*. *Ak4* encodes adenylate kinase 4 (AK4), a protein that localizes to the mitochondrial matrix(83) and is involved in regulating cellular AMP concentrations and, subsequently, the regulation of AMP-sensitive metabolic enzymes such as the AMP-activated Protein Kinase (i.e., AMPK)(84). Thus, like *Ostn*/musclin, AK4 is also associated with adapting tissues to changes in energy availability. In the present study we report that physical activity reduction leads to lower levels of *Ak4* expression in skeletal muscle, an adaptation likely driven by the reduced bioenergetic flux that accompanies physical activity reduction.

Little is known about the function of *Zfhx4*, which encodes zinc finger homeobox 4. *Zfhx4* is highly expressed in developing muscle and proliferating myoblasts, but decreases in expression to very low levels in postnatal skeletal muscles and differentiated myotubes, suggesting its function(s) is/are not critical in tissues with large quantities of postmitotic cells, such as skeletal muscle(85). Indeed, ablation of *Zfhx4* leads to early postnatal lethality linked to respiratory failure, suggesting it plays an important role in early development(86). In colorectal cancer cells, the expression of *Zfhx4* has been computationally associated with the expression of transcripts that promote fatty acid oxidation(87). Thus, considering the known effect of physical inactivity on lowering skeletal muscle fatty acid oxidation(26), and our observation that *Zfhx4* is reduced in expression following physical inactivity, it would not be completely out of line to consider a potential relationship between these processes. Future studies should investigate *Zfhx4* function in postnatal skeletal muscle and determine whether it plays a role in regulating fatty acid oxidation or other functions associated with adapting muscle to changes in bioenergetic demand.

Srrm4os encodes serine/arginine repetitive matrix 4, opposite strand. It exhibits low level expression across most tissues(88), although these screens did not include skeletal muscle which is where we have detected it and found it to be negatively regulated by physical activity reduction. The function of *Srrm4os* is yet to be determined.

In conclusion, although the functional contribution of each of the identified transcripts to the physiology of physical inactivity remains to be determined, this study was a necessary first step toward identifying potential mediators of the physiology associated with activity reduction and sets the stage for similar investigations in other tissues. By acknowledging the need for research animals to be more active than typical laboratory housing permits, but not so active the active period no longer represents activity levels achievable for most humans while also ensuring that both active and inactive control groups are included in the experimental design, we have opened the door to more nuanced investigations into the molecular mechanisms that drive the metabolic impairments associated with physical inactivity. Future studies will provide deeper characterization of the function(s) of each the seven transcripts we identified as being uniquely altered by physical activity reduction in skeletal muscle. It is our hope that such next steps will result in identification of molecular targets that can be exploited for the development of therapeutics capable of supporting metabolism for the many people who cannot meet or sustain a level of physical activity required to protect against disease.

Acknowledgements

We wish to acknowledge past and present members of the Stephenson lab for their contributions, as well as members of the Midwestern University community who contributed to discussions that helped shape the final manuscript. We would also like to acknowledge the Midwestern University Core Facility. This work was supported by a 2022 Midwestern University Faculty Seed Grant (to EJS) and 2022 and 2023 Midwestern University Core Outsourcing Awards (to EJS).

Disclosures

The authors currently have no disclosures, financial or otherwise.

Author contributions

EJS conceived and designed the research. ES, AM, MM, and KM trained the mice. ES, AM, MM, and MJ collected tissues from the mice. EJS, AM, NK, MN, MM, KM, JD, CW performed experiments. EJS, AM, and NK analyzed data. EJS, AM, and NK interpreted results of experiments. EJS prepared the manuscript figures. EJS and NK drafted the manuscript. EJS and AM edited and revised manuscript. All authors approved the submitted version of manuscript.

Supplementary Material

Supplementary File 1 contains the output from the differential gene expression and GSEA analyses.

Data availability

Sequencing files are available at Gene Expression Omnibus (link upon publication). Source data and analysis code are available at https://github.com/esteph16/Inactivity-mediated-molecular-adaptations-1.

Figure legends

Figure 1: Activity reduction model. (a) Experimental design overview. (b) Overview of the graded maximal running test protocol, which was used to determine training speeds and verify performance adaptations at each stage of the study. (c) Overview of the treadmill training protocol. Training sessions occurred 5 d/week with two consecutive days of rest following every five consecutive days of training. (d) Work (J) calculated for individual mice after each of the graded maximal running tests. (e) Body mass of mice across the period of study. (f) Change in body mass between the start of the study and the end of the fourth week and (g) between the fourth week and the end of the study. (h) Mass of the inguinal, retroperitoneal (RP) and gonadal (periuterine and epididymal) adipose depots at the end of the study. (i) Mass of the quadriceps complex (Quad), triceps surae complex, and tibialis anterior skeletal muscle at the end of the study. Values reported are the mean ± standard error with individual values overlaid for n=30 female (n=10 Inactive, n=11 Active, n=9 Activity Reduction) and n=30 male mice (n=10 Inactive, n=10 Active, n=10 Activity Reduction). Data displayed in panels d and e were compared using linear mixed models with likelihood ratio tests. Data displayed in panels f-h were compared using one-way ANOVA with Tukey tests. Data in panel I was either compared by one-way ANOVA (female quadriceps, male triceps surae, male tibialis anterior), or Kruskal-Wallis tests with Dunn tests and Benjamini and Hochberg corrections (female triceps surae, female tibialis anterior, male quadriceps). Inactive group= light grey circles/bars, Active group = dark grey diamonds/bars, Activity Reduction group = red squares/bars.

Figure 2: Effect of activity reduction on energy intake, glucose homeostasis and muscle glycogen stores. (a) Average daily energy intake from food in the final week of the study period. (b) Energy content of stool. (c) Fasting plasma insulin and (d) blood glucose concentrations, and (e) HOMA-IR. (f) Glycogen content of the quadriceps muscles. Values reported are the mean ± standard error with individual values overlaid. Data displayed were compared using one-way ANOVA with Tukey tests where appropriate. The number of biological replicates in each experiment is indicated on each individual panel. Inactive group= light grey circles/bars, Active group = dark grey diamonds/bars, Activity Reduction group = red squares/bars.

Figure 3: Effect of activity reduction on the skeletal muscle (gastrocnemius) transcriptome. Volcano plots demonstrate the number of up- and down-regulated transcripts in (a) the Active compared to Inactive group, (b) the Activity Reduction compared to Inactive group, and (c) the Activity Reduction compared to Active group. Transcripts were considered differentially expressed when $q<0.05$ and expression change was greater than or equal to 20% in either direction compared to the Inactive (a and b) or Active (c) groups. Blue = differentially expressed transcripts with reduced expression, red = differentially expressed transcripts with increased expression, grey = transcripts that are either not differentially expressed or are differentially expressed but do not meet the 20% threshold. (d) Venn diagram showing the overlapping and uniquely expressed transcripts in the Active versus Inactive group (grey), the Activity Reduction versus Inactive group (light red), and the Activity Reduction versus Active group (dark red). (e) Expression of transcripts uniquely changed by Activity Reduction compared to both the Inactive and Active groups. (f) *Igfbp5* expression is decreased in both the Active and Activity Reduction groups compared to the Inactive group. (g) Expression of transcripts uniquely changed by Activity compared to the Inactive and Activity Reduction groups. Values reported are the mean ± standard error with individual values overlaid for n=21 female mice (n=7 Inactive, n=7 Active, n=7 Activity Reduction).

References

1. **Katzmarzyk PT, Friedenreich C, Shiroma EJ, and Lee IM**. Physical inactivity and non-communicable disease burden in low-income, middle-income and high-income countries. *Br J Sports Med* 56: 101-106, 2022.
2. **Strain T, Flaxman S, Guthold R, Semenova E, Cowan M, Riley LM, Bull FC, Stevens GA, and Country Data Author G**. National, regional, and global trends in insufficient physical activity among adults from 2000 to 2022: a pooled analysis of 507 population-based surveys with 5.7 million participants. *Lancet Glob Health* 12: e1232-e1243, 2024.
3. **Bankoski A, Harris TB, McClain JJ, Brychta RJ, Caserotti P, Chen KY, Berrigan D, Troiano RP, and Koster A**. Sedentary activity associated with metabolic syndrome independent of physical activity. *Diabetes Care* 34: 497-503, 2011.
4. **Henson J, Yates T, Biddle SJ, Edwardson CL, Khunti K, Wilmot EG, Gray LJ, Gorely T, Nimmo MA, and Davies MJ**. Associations of objectively measured sedentary behaviour and physical activity with markers of cardiometabolic health. *Diabetologia* 56: 1012-1020, 2013.

5. **Knaeps S, Bourgois JG, Charlier R, Mertens E, Lefevre J, and Wijndaele K**. Ten-year change in sedentary behaviour, moderate-to-vigorous physical activity, cardiorespiratory fitness and cardiometabolic risk: independent associations and mediation analysis. *Br J Sports Med* 52: 1063-1068, 2018.
6. **Wijndaele K, Orrow G, Ekelund U, Sharp SJ, Brage S, Griffin SJ, and Simmons RK**. Increasing objectively measured sedentary time increases clustered cardiometabolic risk: a 6 year analysis of the ProActive study. *Diabetologia* 57: 305-312, 2014.
7. **Ekelund U, Tarp J, Steene-Johannessen J, Hansen BH, Jefferis B, Fagerland MW, Whincup P, Diaz KM, Hooker SP, Chernofsky A, Larson MG, Spartano N, Vasan RS, Dohrn IM, Hagstromer M, Edwardson C, Yates T, Shiroma E, Anderssen SA, and Lee IM**. Dose-response associations between accelerometry measured physical activity and sedentary time and all cause mortality: systematic review and harmonised meta-analysis. *BMJ* 366: l4570, 2019.
8. **Guthold R, Stevens GA, Riley LM, and Bull FC**. Global trends in insufficient physical activity among adolescents: a pooled analysis of 298 population-based surveys with 1.6 million participants. *Lancet Child Adolesc Health* 4: 23-35, 2020.
9. **World Health Organization**. WHO guidelines on physical activity and sedentary behaviour Geneva: 2020.
10. **Guthold R, Stevens GA, Riley LM, and Bull FC**. Worldwide trends in insufficient physical activity from 2001 to 2016: a pooled analysis of 358 population-based surveys with 1.9 million participants. *Lancet Glob Health* 6: e1077-e1086, 2018.
11. **Pedersen MRL, Hansen AF, and Elmose-Osterlund K**. Motives and Barriers Related to Physical Activity and Sport across Social Backgrounds: Implications for Health Promotion. *Int J Environ Res Public Health* 18: 2021.
12. **Lee IM, Shiroma EJ, Lobelo F, Puska P, Blair SN, Katzmarzyk PT, and Lancet Physical Activity Series Working G**. Effect of physical inactivity on major non-communicable diseases worldwide: an analysis of burden of disease and life expectancy. *Lancet* 380: 219-229, 2012.
13. **Chew NWS, Ng CH, Tan DJH, Kong G, Lin C, Chin YH, Lim WH, Huang DQ, Quek J, Fu CE, Xiao J, Syn N, Foo R, Khoo CM, Wang JW, Dimitriadis GK, Young DY, Siddiqui MS, Lam CSP, Wang Y, Figtree GA, Chan MY, Cummings DE, Noureddin M, Wong VW, Ma RCW, Mantzoros CS, Sanyal A, and Muthiah MD**. The global burden of metabolic disease: Data from 2000 to 2019. *Cell Metab* 35: 414-428 e413, 2023.
14. **Lin X, Xu Y, Pan X, Xu J, Ding Y, Sun X, Song X, Ren Y, and Shan PF**. Global, regional, and national burden and trend of diabetes in 195 countries and territories: an analysis from 1990 to 2025. *Sci Rep* 10: 14790, 2020.
15. **DALYs GBD, and Collaborators H**. Global, regional, and national disability-adjusted life-years (DALYs) for 333 diseases and injuries and healthy life expectancy (HALE) for 195 countries and territories, 1990-2016: a systematic analysis for the Global Burden of Disease Study 2016. *Lancet* 390: 1260-1344, 2017.
16. **Pinto AJ, Bergouignan A, Dempsey PC, Roschel H, Owen N, Gualano B, and Dunstan DW**. Physiology of sedentary behavior. *Physiol Rev* 103: 2561-2622, 2023.
17. **Sarto F, Bottinelli R, Franchi MV, Porcelli S, Simunic B, Pisot R, and Narici MV**. Pathophysiological mechanisms of reduced physical activity: Insights from the human step reduction model and animal analogues. *Acta Physiol (Oxf)* 238: e13986, 2023.
18. **Reidy PT, Monnig JM, Pickering CE, Funai K, and Drummond MJ**. Preclinical rodent models of physical inactivity-induced muscle insulin resistance: challenges and solutions. *J Appl Physiol (1985)* 130: 537-544, 2021.
19. **Thyfault JP, and Krogh-Madsen R**. Metabolic disruptions induced by reduced ambulatory activity in free-living humans. *J Appl Physiol (1985)* 111: 1218-1224, 2011.
20. **Krogh-Madsen R, Thyfault JP, Broholm C, Mortensen OH, Olsen RH, Mounier R, Plomgaard P, van Hall G, Booth FW, and Pedersen BK**. A 2-wk reduction of ambulatory activity attenuates peripheral insulin sensitivity. *J Appl Physiol (1985)* 108: 1034-1040, 2010.
21. **Knudsen SH, Hansen LS, Pedersen M, Dejgaard T, Hansen J, Hall GV, Thomsen C, Solomon TP, Pedersen BK, and Krogh-Madsen R**. Changes in insulin sensitivity precede changes in body

composition during 14 days of step reduction combined with overfeeding in healthy young men. *J Appl Physiol (1985)* 113: 7-15, 2012.
22. **McGlory C, von Allmen MT, Stokes T, Morton RW, Hector AJ, Lago BA, Raphenya AR, Smith BK, McArthur AG, Steinberg GR, Baker SK, and Phillips SM**. Failed Recovery of Glycemic Control and Myofibrillar Protein Synthesis With 2 wk of Physical Inactivity in Overweight, Prediabetic Older Adults. *J Gerontol A Biol Sci Med Sci* 73: 1070-1077, 2018.
23. **Bowden Davies KA, Sprung VS, Norman JA, Thompson A, Mitchell KL, Halford JCG, Harrold JA, Wilding JPH, Kemp GJ, and Cuthbertson DJ**. Short-term decreased physical activity with increased sedentary behaviour causes metabolic derangements and altered body composition: effects in individuals with and without a first-degree relative with type 2 diabetes. *Diabetologia* 61: 1282-1294, 2018.
24. **Reidy PT, Yonemura NM, Madsen JH, McKenzie AI, Mahmassani ZS, Rondina MT, Lin YK, Kaput K, and Drummond MJ**. An accumulation of muscle macrophages is accompanied by altered insulin sensitivity after reduced activity and recovery. *Acta Physiol (Oxf)* 226: e13251, 2019.
25. **Rudwill F, O'Gorman D, Lefai E, Chery I, Zahariev A, Normand S, Pagano AF, Chopard A, Damiot A, Laurens C, Hodson L, Canet-Soulas E, Heer M, Meuthen PF, Buehlmeier J, Baecker N, Meiller L, Gauquelin-Koch G, Blanc S, Simon C, and Bergouignan A**. Metabolic Inflexibility Is an Early Marker of Bed-Rest-Induced Glucose Intolerance Even When Fat Mass Is Stable. *J Clin Endocrinol Metab* 103: 1910-1920, 2018.
26. **Shur NF, Simpson EJ, Crossland H, Chivaka PK, Constantin D, Cordon SM, Constantin-Teodosiu D, Stephens FB, Lobo DN, Szewczyk N, Narici M, Prats C, Macdonald IA, and Greenhaff PL**. Human adaptation to immobilization: Novel insights of impacts on glucose disposal and fuel utilization. *J Cachexia Sarcopenia Muscle* 13: 2999-3013, 2022.
27. **Trim WV, Walhin JP, Koumanov F, Turner JE, Shur NF, Simpson EJ, Macdonald IA, Greenhaff PL, and Thompson D**. The impact of physical inactivity on glucose homeostasis when diet is adjusted to maintain energy balance in healthy, young males. *Clin Nutr* 42: 532-540, 2023.
28. **Alibegovic AC, Hojbjerre L, Sonne MP, van Hall G, Stallknecht B, Dela F, and Vaag A**. Impact of 9 days of bed rest on hepatic and peripheral insulin action, insulin secretion, and whole-body lipolysis in healthy young male offspring of patients with type 2 diabetes. *Diabetes* 58: 2749-2756, 2009.
29. **Stephens BR, Granados K, Zderic TW, Hamilton MT, and Braun B**. Effects of 1 day of inactivity on insulin action in healthy men and women: interaction with energy intake. *Metabolism* 60: 941-949, 2011.
30. **Bergouignan A, Schoeller DA, Normand S, Gauquelin-Koch G, Laville M, Shriver T, Desage M, Le Maho Y, Ohshima H, Gharib C, and Blanc S**. Effect of physical inactivity on the oxidation of saturated and monounsaturated dietary Fatty acids: results of a randomized trial. *PLoS Clin Trials* 1: e27, 2006.
31. **Bergouignan A, Trudel G, Simon C, Chopard A, Schoeller DA, Momken I, Votruba SB, Desage M, Burdge GC, Gauquelin-Koch G, Normand S, and Blanc S**. Physical inactivity differentially alters dietary oleate and palmitate trafficking. *Diabetes* 58: 367-376, 2009.
32. **Kump DS, and Booth FW**. Sustained rise in triacylglycerol synthesis and increased epididymal fat mass when rats cease voluntary wheel running. *J Physiol* 565: 911-925, 2005.
33. **Kump DS, and Booth FW**. Alterations in insulin receptor signalling in the rat epitrochlearis muscle upon cessation of voluntary exercise. *J Physiol* 562: 829-838, 2005.
34. **Laye MJ, Thyfault JP, Stump CS, and Booth FW**. Inactivity induces increases in abdominal fat. *J Appl Physiol (1985)* 102: 1341-1347, 2007.
35. **Rector RS, Thyfault JP, Laye MJ, Morris RT, Borengasser SJ, Uptergrove GM, Chakravarthy MV, Booth FW, and Ibdah JA**. Cessation of daily exercise dramatically alters precursors of hepatic steatosis in Otsuka Long-Evans Tokushima Fatty (OLETF) rats. *J Physiol* 586: 4241-4249, 2008.
36. **Teich T, Dunford EC, Porras DP, Pivovarov JA, Beaudry JL, Hunt H, Belanoff JK, and Riddell MC**. Glucocorticoid antagonism limits adiposity rebound and glucose intolerance in young male rats following the cessation of daily exercise and caloric restriction. *Am J Physiol Endocrinol Metab* 311: E56-68, 2016.

37. **Company JM, Roberts MD, Toedebusch RG, Cruthirds CL, and Booth FW**. Sudden decrease in physical activity evokes adipocyte hyperplasia in 70- to 77-day-old rats but not 49- to 56-day-old rats. *Am J Physiol Regul Integr Comp Physiol* 305: R1465-1478, 2013.
38. **Ruegsegger GN, Sevage JA, Childs TE, Grigsby KB, and Booth FW**. 5-Aminoimidazole-4-carboxamide ribonucleotide prevents fat gain following the cessation of voluntary physical activity. *Exp Physiol* 102: 1474-1485, 2017.
39. **Appriou Z, Nay K, Pierre N, Saligaut D, Lefeuvre-Orfila L, Martin B, Cavey T, Ropert M, Loreal O, Rannou-Bekono F, and Derbre F**. Skeletal muscle ceramides do not contribute to physical-inactivity-induced insulin resistance. *Appl Physiol Nutr Metab* 44: 1180-1188, 2019.
40. **Siripoksup P, Cao G, Cluntun AA, Maschek JA, Pearce Q, Lang MJ, Jeong MY, Eshima H, Ferrara PJ, Opurum PC, Mahmassani ZS, Peterlin AD, Watanabe S, Walsh MA, Taylor EB, Cox JE, Drummond MJ, Rutter J, and Funai K**. Sedentary behavior in mice induces metabolic inflexibility by suppressing skeletal muscle pyruvate metabolism. *J Clin Invest* 2024.
41. **Roemers P, Hulst Y, van Heijningen S, van Dijk G, van Heuvelen MJG, De Deyn PP, and van der Zee EA**. Inducing Physical Inactivity in Mice: Preventing Climbing and Reducing Cage Size Negatively Affect Physical Fitness and Body Composition. *Front Behav Neurosci* 13: 221, 2019.
42. **Mahmassani ZS, Reidy PT, McKenzie AI, Petrocelli JJ, Matthews O, de Hart NM, Ferrara PJ, O'Connell RM, Funai K, and Drummond MJ**. Absence of MyD88 from Skeletal Muscle Protects Female Mice from Inactivity-Induced Adiposity and Insulin Resistance. *Obesity (Silver Spring)* 28: 772-782, 2020.
43. **Fushiki T, Kano T, Inoue K, and Sugimoto E**. Decrease in muscle glucose transporter number in chronic physical inactivity in rats. *Am J Physiol* 260: E403-410, 1991.
44. **Martin B, Ji S, Maudsley S, and Mattson MP**. "Control" laboratory rodents are metabolically morbid: why it matters. *Proc Natl Acad Sci U S A* 107: 6127-6133, 2010.
45. **McLean AC, Valenzuela N, Fai S, and Bennett SA**. Performing vaginal lavage, crystal violet staining, and vaginal cytological evaluation for mouse estrous cycle staging identification. *J Vis Exp* e4389, 2012.
46. **Aranda PS, LaJoie DM, and Jorcyk CL**. Bleach gel: a simple agarose gel for analyzing RNA quality. *Electrophoresis* 33: 366-369, 2012.
47. **Community TG**. The Galaxy platform for accessible, reproducible, and collaborative data analyses: 2024 update. *Nucleic Acids Research* 52: W83-W94, 2024.
48. **Chen S, Zhou Y, Chen Y, and Gu J**. fastp: an ultra-fast all-in-one FASTQ preprocessor. *Bioinformatics* 34: i884-i890, 2018.
49. **Dobin A, Davis CA, Schlesinger F, Drenkow J, Zaleski C, Jha S, Batut P, Chaisson M, and Gingeras TR**. STAR: ultrafast universal RNA-seq aligner. *Bioinformatics* 29: 15-21, 2012.
50. **Liao Y, Smyth GK, and Shi W**. featureCounts: an efficient general purpose program for assigning sequence reads to genomic features. *Bioinformatics* 30: 923-930, 2013.
51. **Sergushichev AA**. An algorithm for fast preranked gene set enrichment analysis using cumulative statistic calculation. *bioRxiv* 060012, 2016.
52. **Subramanian A, Tamayo P, Mootha VK, Mukherjee S, Ebert BL, Gillette MA, Paulovich A, Pomeroy SL, Golub TR, Lander ES, and Mesirov JP**. Gene set enrichment analysis: a knowledge-based approach for interpreting genome-wide expression profiles. *Proc Natl Acad Sci U S A* 102: 15545-15550, 2005.
53. **Castanza AS, Recla JM, Eby D, Thorvaldsdottir H, Bult CJ, and Mesirov JP**. Extending support for mouse data in the Molecular Signatures Database (MSigDB). *Nat Methods* 20: 1619-1620, 2023.
54. **Liberzon A, Subramanian A, Pinchback R, Thorvaldsdottir H, Tamayo P, and Mesirov JP**. Molecular signatures database (MSigDB) 3.0. *Bioinformatics* 27: 1739-1740, 2011.
55. **Wickham H, Averick, Mara , Bryan J, Chang W, D'Agostino McGowan L, François R, Grolemund G, Hayes A, Henry L, Hester J, Kuhn M, Lin Pedersen T, Miller E, Milton Bache S, Müller K, Ooms J, Robinson D, Seidel DP, Spinu V, Takahashi K, Vaughan D, Wilke C, Woo K, and Yutani H**. Welcome to the Tidyverse. *Journal of Open Source Software* 4: 1686, 2019.
56. **Fox J, and Weisberg S**. *An R Companion to Applied Regression*. Thousand Oaks CA: Sage, 2019.

57. **Mangiafico S**. rcompanion: Functions to Support Extension Education Program Evaluation. New Brunswick, New Jersey: 2024.
58. **Kassambara A**. rstatix: Pipe-Friendly Framework for Basic Statistical Tests. 2023.
59. **Bates D, Maechler M, Bolker B, and Walker S**. Fitting Linear Mixed-Effects Models Using lme4. *Journal of Statistical Software* 67: 1-48, 2015.
60. **Lenth RV, Bolker B, Buerkner P, Giné-Vázquez I, Herve M, Jung M, Love J, Miguez F, Piaskowski J, Riebl H, and Singmann H**. emmeans: Estimated Marginal Means, aka Least-Squares Means. 2024.
61. **Eggelbusch M, Charlton BT, Bosutti A, Ganse B, Giakoumaki I, Grootemaat AE, Hendrickse PW, Jaspers Y, Kemp S, Kerkhoff TJ, Noort W, van Weeghel M, van der Wel NN, Wesseling JR, Frings-Meuthen P, Rittweger J, Mulder ER, Jaspers RT, Degens H, and Wust RCI**. The impact of bed rest on human skeletal muscle metabolism. *Cell Rep Med* 5: 101372, 2024.
62. **Tsai AC, Bach J, and Borer KT**. Somatic, endocrine, and serum lipid changes during detraining in adult hamsters. *Am J Clin Nutr* 34: 373-376, 1981.
63. **Rueda-Robles A, Audano M, Alvarez-Mercado AI, and Rubio-Tomas T**. Functions of SMYD proteins in biological processes: What do we know? An updated review. *Arch Biochem Biophys* 712: 109040, 2021.
64. **Diehl F, Brown MA, van Amerongen MJ, Novoyatleva T, Wietelmann A, Harriss J, Ferrazzi F, Bottger T, Harvey RP, Tucker PW, and Engel FB**. Cardiac deletion of Smyd2 is dispensable for mouse heart development. *PLoS One* 5: e9748, 2010.
65. **Donlin LT, Andresen C, Just S, Rudensky E, Pappas CT, Kruger M, Jacobs EY, Unger A, Zieseniss A, Dobenecker MW, Voelkel T, Chait BT, Gregorio CC, Rottbauer W, Tarakhovsky A, and Linke WA**. Smyd2 controls cytoplasmic lysine methylation of Hsp90 and myofilament organization. *Genes Dev* 26: 114-119, 2012.
66. **Dang K, Farooq HMU, Dong J, Yang H, Kong Y, Wang H, Jiang S, Gao Y, and Qian A**. Transcriptomic and proteomic time-course analyses based on Metascape reveal mechanisms against muscle atrophy in hibernating Spermophilus dauricus. *Comp Biochem Physiol A Mol Integr Physiol* 275: 111336, 2023.
67. **Watts AJ, and Storey KB**. Hibernation impacts lysine methylation dynamics in the 13-lined ground squirrel, Ictidomys tridecemlineatus. *J Exp Zool A Ecol Integr Physiol* 331: 234-244, 2019.
68. **Wang Z, Zhu S, Jia Y, Wang Y, Kubota N, Fujiwara N, Gordillo R, Lewis C, Zhu M, Sharma T, Li L, Zeng Q, Lin YH, Hsieh MH, Gopal P, Wang T, Hoare M, Campbell P, Hoshida Y, and Zhu H**. Positive selection of somatically mutated clones identifies adaptive pathways in metabolic liver disease. *Cell* 186: 1968-1984 e1920, 2023.
69. **Wang Y, Jin G, Guo Y, Cao Y, Niu S, Fan X, and Zhang J**. SMYD2 suppresses p53 activity to promote glucose metabolism in cervical cancer. *Exp Cell Res* 404: 112649, 2021.
70. **Wang Q, Cao DH, Jin CL, Lin CK, Ma HW, and Wu YY**. A method of utrophin up-regulation through RNAi-mediated knockdown of the transcription factor EN1. *J Int Med Res* 39: 161-171, 2011.
71. **Gyorfi AH, Matei AE, Fuchs M, Liang C, Rigau AR, Hong X, Zhu H, Luber M, Bergmann C, Dees C, Ludolph I, Horch RE, Distler O, Wang J, Bengsch B, Schett G, Kunz M, and Distler JHW**. Engrailed 1 coordinates cytoskeletal reorganization to induce myofibroblast differentiation. *J Exp Med* 218: 2021.
72. **Mascharak S, desJardins-Park HE, Davitt MF, Griffin M, Borrelli MR, Moore AL, Chen K, Duoto B, Chinta M, Foster DS, Shen AH, Januszyk M, Kwon SH, Wernig G, Wan DC, Lorenz HP, Gurtner GC, and Longaker MT**. Preventing Engrailed-1 activation in fibroblasts yields wound regeneration without scarring. *Science* 372: 2021.
73. **Ma X, Zhao LL, Yu YC, and Cheng Y**. Engrailed: Pathological and physiological effects of a multifunctional developmental gene. *Genesis* 62: e23557, 2024.
74. **Zhang C, Weng Y, Shi F, and Jin W**. The Engrailed-1 Gene Stimulates Brown Adipogenesis. *Stem Cells Int* 2016: 7369491, 2016.
75. **Shmuel-Galia L, Humphries F, Vierbuchen T, Jiang Z, Santos N, Johnson J, Shklyar B, Joannas L, Mustone N, Sherman S, Ward D, Houghton J, Baer CE, O'Hara A, Henao-Mejia J, Hoebe K, and Fitzgerald KA**. The lncRNA HOXA11os regulates mitochondrial function in myeloid cells to maintain intestinal homeostasis. *Cell Metab* 35: 1441-1456 e1449, 2023.

76. **Nishizawa H, Matsuda M, Yamada Y, Kawai K, Suzuki E, Makishima M, Kitamura T, and Shimomura I**. Musclin, a novel skeletal muscle-derived secretory factor. *J Biol Chem* 279: 19391-19395, 2004.
77. **Subbotina E, Sierra A, Zhu Z, Gao Z, Koganti SR, Reyes S, Stepniak E, Walsh SA, Acevedo MR, Perez-Terzic CM, Hodgson-Zingman DM, and Zingman LV**. Musclin is an activity-stimulated myokine that enhances physical endurance. *Proc Natl Acad Sci U S A* 112: 16042-16047, 2015.
78. **Jin L, Han S, Lv X, Li X, Zhang Z, Kuang H, Chen Z, Lv CA, Peng W, Yang Z, Yang M, Mi L, Liu T, Ma S, Qiu X, Wang Q, Pan X, Shan P, Feng Y, Li J, Wang F, Xie L, Zhao X, Fu JF, Lin JD, and Meng ZX**. The muscle-enriched myokine Musclin impairs beige fat thermogenesis and systemic energy homeostasis via Tfr1/PKA signaling in male mice. *Nat Commun* 14: 4257, 2023.
79. **Chen WJ, Liu Y, Sui YB, Yang HT, Chang JR, Tang CS, Qi YF, Zhang J, and Yin XH**. Positive association between musclin and insulin resistance in obesity: evidence of a human study and an animal experiment. *Nutr Metab (Lond)* 14: 46, 2017.
80. **Shimomura M, Horii N, Fujie S, Inoue K, Hasegawa N, Iemitsu K, Uchida M, and Iemitsu M**. Decreased muscle-derived musclin by chronic resistance exercise is associated with improved insulin resistance in rats with type 2 diabetes. *Physiol Rep* 9: e14823, 2021.
81. **Chen WJ, Liu Y, Sui YB, Zhang B, Zhang XH, and Yin XH**. Increased circulating levels of musclin in newly diagnosed type 2 diabetic patients. *Diab Vasc Dis Res* 14: 116-121, 2017.
82. **Harris MP, Zeng S, Zhu Z, Lira VA, Yu L, Hodgson-Zingman DM, and Zingman LV**. Myokine Musclin Is Critical for Exercise-Induced Cardiac Conditioning. *Int J Mol Sci* 24: 2023.
83. **Noma T, Fujisawa K, Yamashiro Y, Shinohara M, Nakazawa A, Gondo T, Ishihara T, and Yoshinobu K**. Structure and expression of human mitochondrial adenylate kinase targeted to the mitochondrial matrix. *Biochem J* 358: 225-232, 2001.
84. **Lanning NJ, Looyenga BD, Kauffman AL, Niemi NM, Sudderth J, DeBerardinis RJ, and MacKeigan JP**. A mitochondrial RNAi screen defines cellular bioenergetic determinants and identifies an adenylate kinase as a key regulator of ATP levels. *Cell Rep* 7: 907-917, 2014.
85. **Kostich WA, and Sanes JR**. Expression of zfh-4, a new member of the zinc finger-homeodomain family, in developing brain and muscle. *Dev Dyn* 202: 145-152, 1995.
86. **Zhang M, Du S, Ou H, Cui R, Jiang N, Lin Y, Ge R, Ma D, and Zhang J**. Ablation of Zfhx4 results in early postnatal lethality by disrupting the respiratory center in mice. *J Mol Cell Biol* 13: 210-224, 2021.
87. **Zou P, Chen C, and Wu X**. Identification of fatty acid oxidation-related subtypes by integrated analysis of bulk- and single-cell transcriptome profiling in colorectal cancer. *J Gastrointest Oncol* 15: 147-163, 2024.
88. **Yue F, Cheng Y, Breschi A, Vierstra J, Wu W, Ryba T, Sandstrom R, Ma Z, Davis C, Pope BD, Shen Y, Pervouchine DD, Djebali S, Thurman RE, Kaul R, Rynes E, Kirilusha A, Marinov GK, Williams BA, Trout D, Amrhein H, Fisher-Aylor K, Antoshechkin I, DeSalvo G, See LH, Fastuca M, Drenkow J, Zaleski C, Dobin A, Prieto P, Lagarde J, Bussotti G, Tanzer A, Denas O, Li K, Bender MA, Zhang M, Byron R, Groudine MT, McCleary D, Pham L, Ye Z, Kuan S, Edsall L, Wu YC, Rasmussen MD, Bansal MS, Kellis M, Keller CA, Morrissey CS, Mishra T, Jain D, Dogan N, Harris RS, Cayting P, Kawli T, Boyle AP, Euskirchen G, Kundaje A, Lin S, Lin Y, Jansen C, Malladi VS, Cline MS, Erickson DT, Kirkup VM, Learned K, Sloan CA, Rosenbloom KR, Lacerda de Sousa B, Beal K, Pignatelli M, Flicek P, Lian J, Kahveci T, Lee D, Kent WJ, Ramalho Santos M, Herrero J, Notredame C, Johnson A, Vong S, Lee K, Bates D, Neri F, Diegel M, Canfield T, Sabo PJ, Wilken MS, Reh TA, Giste E, Shafer A, Kutyavin T, Haugen E, Dunn D, Reynolds AP, Neph S, Humbert R, Hansen RS, De Bruijn M, Selleri L, Rudensky A, Josefowicz S, Samstein R, Eichler EE, Orkin SH, Levasseur D, Papayannopoulou T, Chang KH, Skoultchi A, Gosh S, Disteche C, Treuting P, Wang Y, Weiss MJ, Blobel GA, Cao X, Zhong S, Wang T, Good PJ, Lowdon RF, Adams LB, Zhou XQ, Pazin MJ, Feingold EA, Wold B, Taylor J, Mortazavi A, Weissman SM, Stamatoyannopoulos JA, Snyder MP, Guigo R, Gingeras TR, Gilbert DM, Hardison RC, Beer MA, Ren B, and Mouse EC**. A comparative encyclopedia of DNA elements in the mouse genome. *Nature* 515: 355-364, 2014.

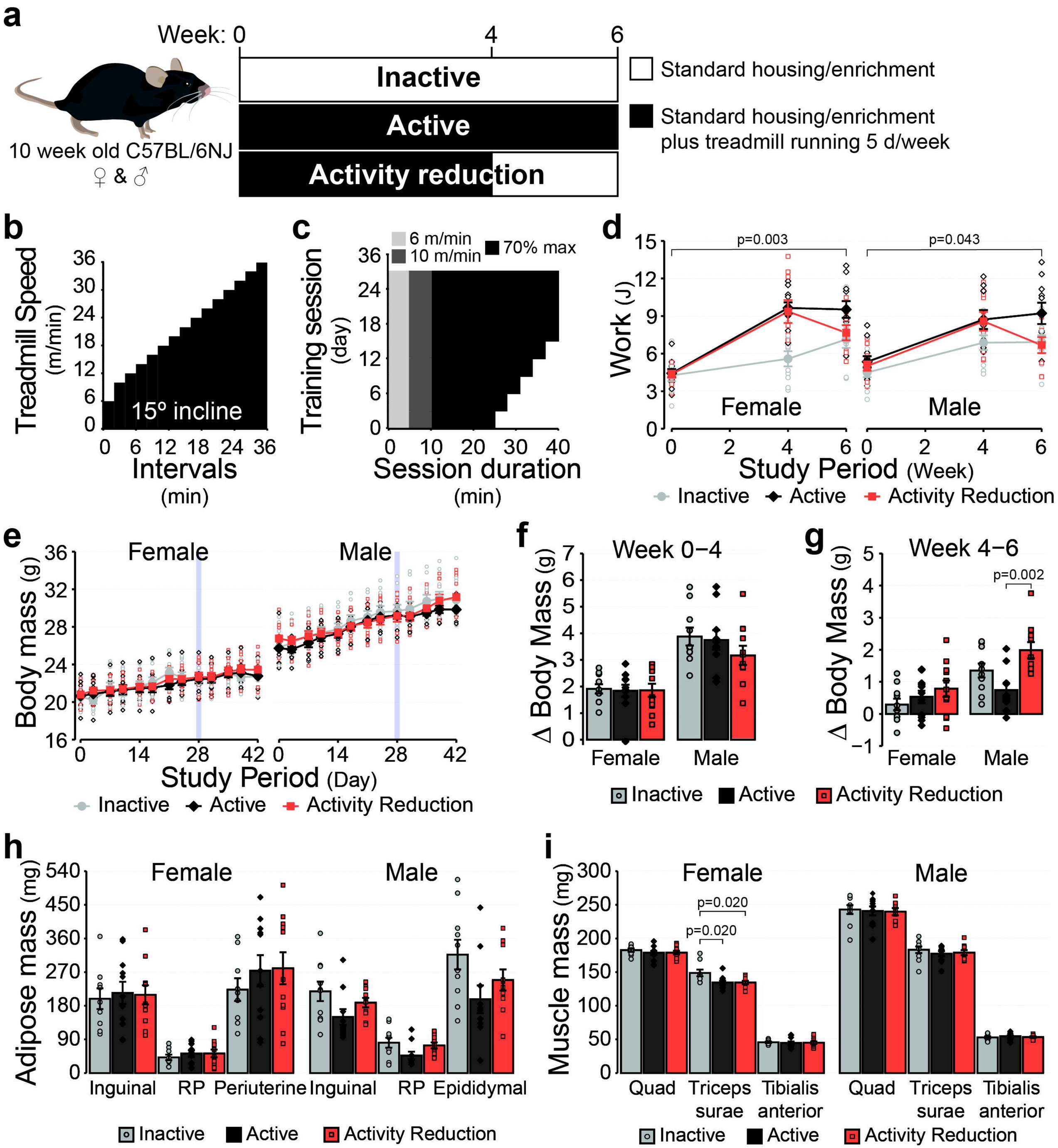
a
Week: 0
4
6
10 week old C57BL/6NJ
♀ & ♂
Inactive
Active
Activity reduction
Standard housing/enrichment
Standard housing/enrichment plus treadmill running 5 d/week
b
Treadmill Speed (m/min)
15º incline
Intervals (min)
c
Training session (day)
6 m/min
10 m/min
70% max
Session duration (min)
d
Work (J)
p=0.003
p=0.043
Female
Male
Study Period (Week)
Inactive
Active
Activity Reduction
e
Body mass (g)
Female
Male
Study Period (Day)
Inactive
Active
Activity Reduction
f
Week 0–4
Δ Body Mass (g)
Female
Male
g
Week 4–6
Δ Body Mass (g)
p=0.002
Female
Male
Inactive
Active
Activity Reduction
h
Adipose mass (mg)
Female
Male
Inguinal
RP
Periuterine
Inguinal
RP
Epididymal
Inactive
Active
Activity Reduction
i
Muscle mass (mg)
Female
Male
p=0.020
p=0.020
Quad
Triceps surae
Tibialis anterior
Quad
Triceps surae
Tibialis anterior
Inactive
Active
Activity Reduction

Figure 1

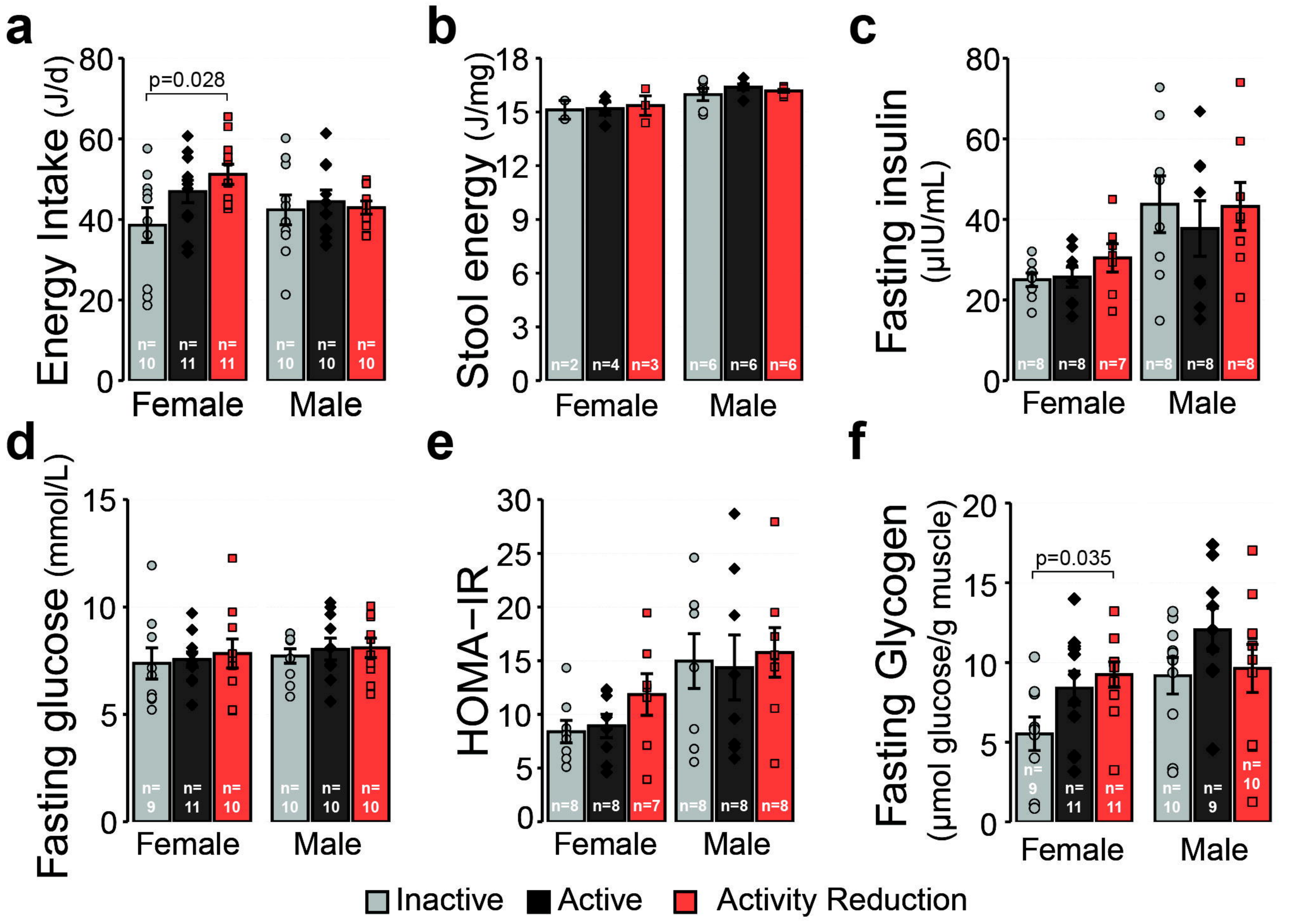
a
Energy Intake (J/d)
p=0.028
n= 10
n= 11
n= 11
n= 10
n= 10
n= 10
Female
Male
b
Stool energy (J/mg)
n=2
n=4
n=3
n=6
n=6
n=6
Female
Male
c
Fasting insulin (µIU/mL)
n=8
n=8
n=7
n=8
n=8
n=8
Female
Male
d
Fasting glucose (mmol/L)
n= 9
n= 11
n= 10
n= 10
n= 10
n= 10
Female
Male
e
HOMA-IR
n=8
n=8
n=7
n=8
n=8
n=8
Female
Male
f
Fasting Glycogen (µmol glucose/g muscle)
p=0.035
n= 9
n= 11
n= 11
n= 10
n= 9
n= 10
Female
Male
Inactive
Active
Activity Reduction

Figure 2

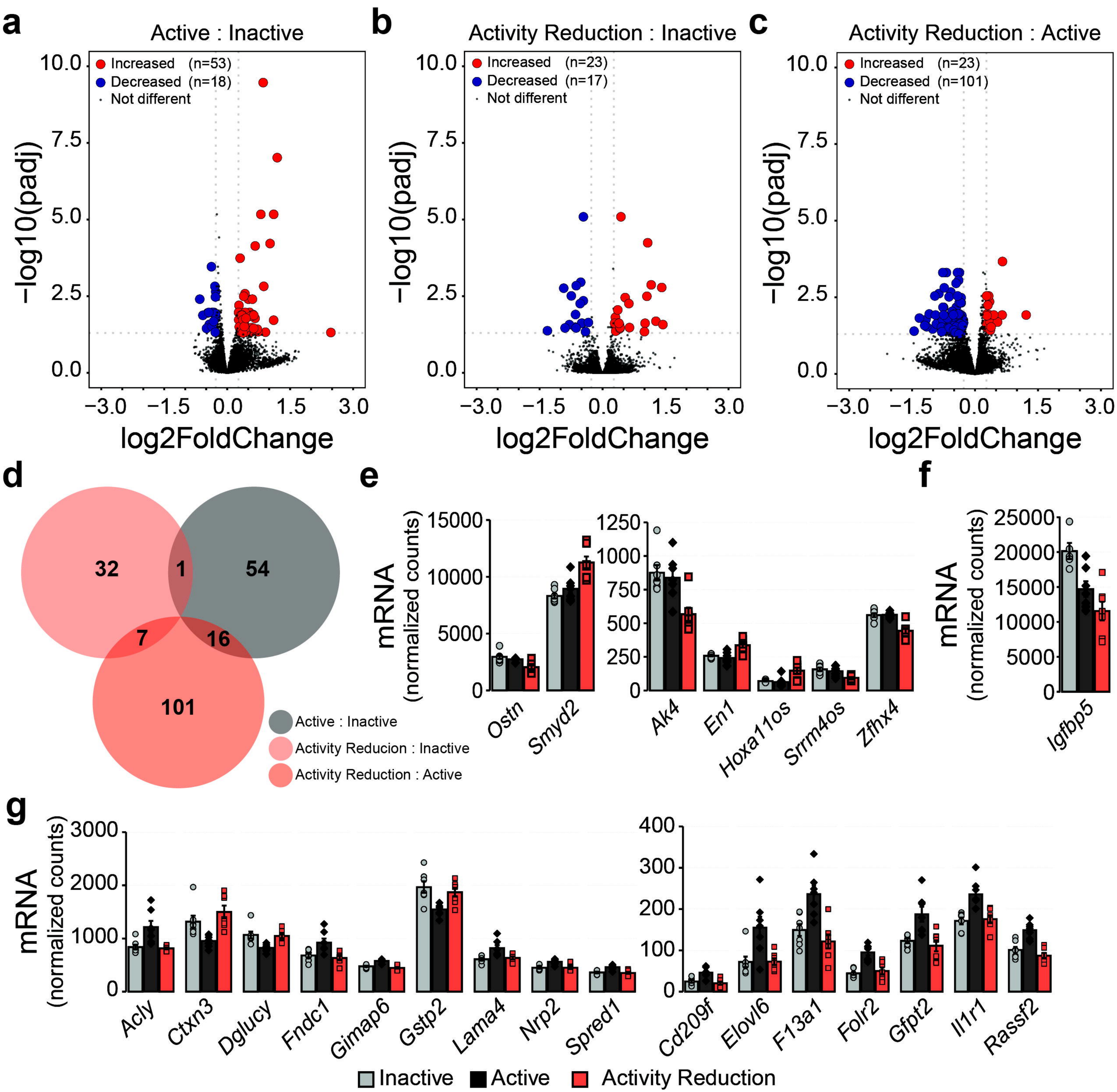
a
Active : Inactive
Increased (n=53)
Decreased (n=18)
Not different
−log10(padj)
log2FoldChange
b
Activity Reduction : Inactive
Increased (n=23)
Decreased (n=17)
Not different
c
Activity Reduction : Active
Increased (n=23)
Decreased (n=101)
Not different
d
32
1
54
7
16
101
Active : Inactive
Activity Reducion : Inactive
Activity Reduction : Active
e
mRNA (normalized counts)
Ostn
Smyd2
Ak4
En1
Hoxa11os
Srrm4os
Zfhx4
f
Igfbp5
g
Acly
Ctxn3
Dglucy
Fndc1
Gimap6
Gstp2
Lama4
Nrp2
Spred1
Cd209f
Elovl6
F13a1
Folr2
Gfpt2
Il1r1
Rassf2
Inactive
Active
Activity Reduction

Figure 3